ORIGINAL ARTICLE

Alcohol dependence decreases functional activation of the caudate nucleus during model-based decision processes

Amadeus Magrabi[1,2] | Anne Beck[3] | Daniel J. Schad[3] | Tristram A. Lett[1] | Christian M. Stoppel[1] | Katrin Charlet[1,4] | Falk Kiefer[5] | Andreas Heinz[1] | Henrik Walter[1,2]

[1]Department of Psychiatry and Psychotherapy, Charité – Universitätsmedizin Berlin, Berlin, Germany

[2]Berlin School of Mind and Brain, Humboldt-Universität zu Berlin, Berlin, Germany

[3]HMU Health and Medical University Potsdam, Potsdam, Germany

[4]Section on Clinical Genomics and Experimental Therapeutics, National Institute on Alcohol Abuse and Alcoholism, National Institutes of Health, Bethesda, Maryland, USA

[5]Department of Addictive Behavior and Addiction Medicine, Medical Faculty Mannheim, Central Institute of Mental Health, Heidelberg University, Mannheim, Germany

Correspondence
Amadeus Magrabi, Division of Mind and Brain Research, Department of Psychiatry and Psychotherapy, Charité – Universitätsmedizin Berlin, Charitéplatz 1, 10117 Berlin, Germany.
Email: amadeus.magrabi@gmail.com

Funding information
Berlin School of Mind and Brain; Charité Berlin; Ministry of Education and Research, Grant/Award Number: 01ZX1311E/e and 01EE1406A; Canadian Institute of Health Research; German Research Foundation, Grant/Award Number: Exc 257, HE2597/14-2, 402170461, TRR 265 and 1936/1-1

Abstract

Background: Impaired decision making, a key characteristic of alcohol dependence (AD), manifests in continuous alcohol consumption despite severe negative consequences. The neural basis of this impairment in individuals with AD and differences with known neural decision mechanisms among healthy subjects are not fully understood. In particular, it is unclear whether the choice behavior among individuals with AD is based on a general impairment of decision mechanisms or is mainly explained by altered value attribution, with an overly high subjective value attributed to alcohol-related stimuli.

Methods: Here, we use a functional magnetic resonance imaging (fMRI) monetary reward task to compare the neural processes of model-based decision making and value computation between AD individuals ($n = 32$) and healthy controls ($n = 32$). During fMRI, participants evaluated monetary offers with respect to dynamically changing constraints and different levels of uncertainty.

Results: Individuals with AD showed lower activation associated with model-based decision processes in the caudate nucleus than controls, but there were no group differences in value-related neural activity or task performance.

Conclusions: Our findings highlight the role of the caudate nucleus in impaired model-based decisions of alcohol-dependent individuals.

KEYWORDS
alcohol, computational modeling, decision making, fMRI, value

---

INTRODUCTION

Alcohol dependence (AD) is a highly prevalent psychiatric disorder, accounting for about 3 million deaths per year worldwide (World Health Organization, 2018). It is characterized by a loss of control over the consumption of alcohol, a negative emotional state (such as anxiety) during withdrawal, and continued drinking despite repeated harmful consequences (Everitt & Robbins, 2005; Koob & Volkow, 2010).

Regarding the neurobiological basis of addiction, multiple studies have investigated the neural response of AD patients to alcoholic stimuli and related conditioning processes (Beck et al., 2012; Chase et al., 2011; Kühn & Gallinat, 2011; Schad et al., 2019) indicating an increased incentive salience and value attribution to those cues (Wrase et al., 2007) as well as aberrant processing of nonalcoholic stimuli, in terms of diminished responsiveness toward nonalcoholic reinforcements (Goldstein & Volkow, 2011; Luijten et al., 2017; Schacht et al., 2013; Sebold et al., 2017). However, it was also observed that substance use disorders were associated with increased limbic system sensitivity to reward and loss delivery (Bjork et al., 2008).

A further important and putatively related aspect of addictive disorders are maladaptive choices that oppose the explicitly stated desires of the patients, such as continuing consumption despite the desire to abstain. Here, two extensively explored components of decision making are of importance that have been characterized using computational modeling methods: (1) a flexible planning system integrating all available information to find the most appropriate decision and considering the consequences of actions: the goal-directed or model-based system and (2) a rigid habitual system that simply repeats actions that were rewarded in the past without taking a model of the environment into account: the habitual or model-free system (e.g., see Sebold et al., 2014). In addictive behaviors, it was observed that there is a shift from goal-directed (i.e., model-based) toward habitual (model-free) decision making (e.g., Voon et al., 2017). On the neuronal level, it has been suggested that AD develops through a systematic shift in the neural systems that regulate behavior, with increased involvement of the dorsolateral striatum/putamen (in rodents/humans) controlling habitual behavior, and decreased involvement of the dorsomedial striatum/caudate controlling flexible and goal-directed behavior (Corbit et al., 2012; DePoy et al., 2013; Everitt & Wolf, 2002; Furlong et al., 2014; Gahnstrom & Spiers, 2020; Geerts et al., 2020; Sharpe et al., 2019; Vollstädt-Klein et al., 2010). In rodent studies, it has been shown that lesions of the dorsomedial striatum (comparable to human's caudate) block goal-directed behavior (Yin et al., 2005), while in contrast, lesions of the dorsolateral striatum (comparable to human's putamen) disrupt habit formation (Yin et al., 2004). Thus, the capacity for decision making in terms of goal-directed behavior seems to be a core function affected in AD (Mollick & Kober, 2020; Sebold et al., 2014). In particular, AD patients continuously choose to consume alcohol and neglect the long-term consequences of sustained consumption on their physical and psychological health (Amlung et al., 2017; Phung et al., 2019).

Other studies suggest that the choice behavior of AD patients (Kamarajan et al., 2020; Rubio et al., 2008; Virkkunen, 1994) is based on an overactive neural value system (Arcurio et al., 2015; Goldstein & Volkow, 2011; Seo et al., 2013), which has been associated with ventromedial prefrontal cortex (vmPFC; Bartra et al., 2013; Clithero & Rangel, 2014; Lee et al., 2021). However, it is not well understood how exactly and under what conditions these shifts in neural information processing can occur.

Here, we developed a sequential decision-making task to investigate this process in AD patients and healthy control subjects via functional magnetic resonance imaging (fMRI). To detect behavioral and neural differences between AD patients and controls, we designed a task that specifically relies on the ability to flexibly adapt choices to multiple factors and their associated consequences. To further contribute to the core question of whether AD affects decision networks in general, beyond choices that are specifically related to alcohol, we used a task that relies on monetary incentives instead of alcoholic stimuli.

In this decision task, participants had to decide whether to accept or reject various monetary offers that were presented to them. Crucially, for each experimental block of 20 offers, participants were only allowed to accept a maximum of 5 offers. To make optimal choices and maximize the probability of accepting only the highest offers in a block, participants thus had to consider three factors: (1) the value of the current offer, (2) the number of offers that can still be accepted before reaching the limit, and (3) the number of offers that are remaining in the current block. These parameters were included in a decision model (Economides et al., 2014) and computed for the choice data. Parameter estimates of the model were then used as parametric modulators in the analysis of the functional MRI data to identify brain regions that compute model-based decision processes, and to test for putative differences between AD patients and controls.

Based on previous studies, we defined regions of interest (ROIs) and hypothesized that AD patients would show (1) a decreased representation of model-based decision processes in caudate nucleus and (2) an increased representation of decision value in vmPFC.

MATERIALS AND METHODS

Participants

The experimental sample consisted of 32 detoxified AD patients and 32 healthy control subjects (Table 1). The sample was acquired as part of the *National Genome Research Network* (Spanagel et al., 2010) at *Charité—Universitätsmedizin Berlin*. All subjects were right-handed, had a normal or corrected-to-normal vision, and provided informed consent before participation. AD patients were diagnosed with AD according to DSM-IV and ICD-10

TABLE 1 Descriptive statistics of alcohol-dependent patients and healthy control subjects

	AD patients (22 male, 10 female)			Control subjects (23 male, nine female)			Group difference	
	Mean	SD	Missing data	Mean	SD	Missing data	p	T
Lifetime drinking history (consumption in kg)	909.9	885.6	2	83.8	99	0	<0.01[a]	−5.2
Education level[a]	Median: 2	IQR: 1	0	Median: 3	IQR: 1	0	M-W U-test: 0.137	Z-value: −1.49
Age	46.5	8.9	0	38.9	10.5	0	<0.01[a]	−3.13
Pack years of cigarette consumption[b]	21.6	18.1	0	9.6	14.7	0	<0.01[a]	−2.9
Number of smokers	25	–	0	10	–	0	–	–
Duration of dependence (years)	6.6	5.6	4	–	–	–	–	–
Age of dependence onset	40.8	7.8	4	–	–	–	–	–
Percentage of invalid trials[c]	24.27	9.40	0	25.12	6.91	0	0.68	0.41

Abbreviations: AD, alcohol dependence; IQR, interquartile range; M-W U-test, Mann–Whitney U-test; SD, standard deviation.

[a]Ordinal variable corresponding to education levels in the German school system (from lowest to highest): 0 = no graduation, 1 = *Hauptschule*, 2 = *Realschule*, 3 = *Abitur*.

[b]Definition of pack years: ((number of consumed cigarettes per day/18) × c number of years smoked), with 18 as the standard amount of cigarettes in one pack.

[c]Definition of invalid trials: maximum number of offers were already accepted or no response was given in time.
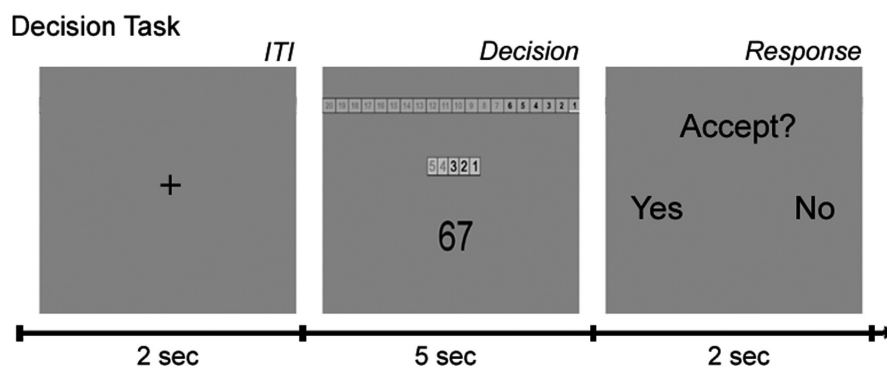

FIGURE 1 Trial structure of the decision task. In the decision phase, participants were presented with offer values (in cents) as well as indicators for the remaining number of trials (maximum of 20 for each of the nine blocks) and for the number of offers that can still be accepted (maximum of five in each block). In the response phase, participants specified their choice to accept or reject an offer with their left or right index finger. ITI, inter-trial interval

(Diagnostic and Statistical Manual of Mental Disorders, Fourth Edition (DSM-IV), Structured Clinical Interview for DSM-IV Axis I Disorders (SCID-I); First et al., 2001) and completed medically supervised detoxification (mean detoxification days when data was acquired: 12.71 ± 4.93 SD). Exclusion criteria for all participants were DSM-IV Axis-I disorders (excluding alcohol and nicotine dependence in AD patients, and excluding only nicotine dependence in control subjects), use of cannabinoids, benzodiazepines, barbiturates, cocaine, amphetamines, opiates (tested by urine screening) or psychotropic medication, claustrophobia, epilepsy, other neurological or psychiatric illnesses, and pregnancy. Data sets of subjects that showed excessive head motion in the scanner or failed to follow task instructions (i.e., subjects that continuously tried to accept offers even though the acceptance limit was already reached) were excluded from further analyses. The amount of lifetime alcohol consumption was assessed using the Lifetime Drinking History (Skinner & Sheu, 1982) and the experiment was approved by the local ethics committee.

Group comparisons revealed a difference with respect to age (Table 1), which was controlled for by including age as a covariate in statistical analyses of group differences. Further, as is commonly found in studies on AD patients (Batel et al., 2006), patients showed increased smoking behavior (Table 1) as indicated by pack years of cigarette consumption (definition of pack years: (number of consumed cigarettes per day/18) × number of years smoked; with 18 as the standard amount of cigarettes in one pack). Since cigarette consumption was significantly correlated with lifetime alcohol intake in AD patients ($r = 0.52$, $p = 0.003$), and can therefore interfere with

variance related to AD in statistical analyses, pack years of cigarette consumption were not included as a covariate in our analyses.

Task

The decision task was implemented in Presentation software (Neurobehavioral Systems) and consisted of nine blocks including 20 trials each. During each trial, participants had to decide whether to accept or reject a monetary offer between 1 and 99 cents (€). However, they were only allowed to accept a maximum of five out of 20 offers in each block. The main challenge of the task was thus to evaluate whether one should accept offers in early trials or one should wait instead for potentially higher offers in later trials. To allow for strategic decision making and rough estimates of upcoming monetary offers, consecutive offers never exceeded a value difference of more than 11 cents, with possible value changes being taken from the set [−11, −7, −3, 3, 7, 11]. Unknown to participants, the sequences of monetary offers followed a predefined pattern for each block (Figure S1), but the order in which participants were presented with block-specific patterns was randomized between participants.

Participants could base their decision whether to accept or reject a given offer on primarily three factors: (1) *offer value*, indicating the monetary amount of the current offer, (2) *offer index*, indicating how many offers were already presented in a block, and (3) the *number of accepts*, indicating how many offers were already accepted in a block. Information about the current state of these three factors was presented to participants in each trial for 5 s (Figure 1). After that, in a separate response phase (2 s), participants had to indicate their choice to accept or reject the offer via button presses with their left or right index finger. When the choice was not indicated within the time limit of 2 s, the offer was counted as rejected. The inter-trial interval consisted of a simple fixation cross and lasted for 2 s. Every block ended with a feedback screen (5 s), indicating the monetary earnings of the respective block, and an empty pause screen (10 s), in which participants could prepare for the next block.

Computational model

The decisions in the task allowed for strategic use of the variables offer value, offer index, and the number of accepts. To estimate to what extent participants took these variables into account, instead of basing their choices solely on the offer value, a decision model that has been validated for a similar sequential decision task (Economides et al., 2014) was computed for the choice data. The model estimates the expected value of accepting an offer V_A by comparing the monetary offer value R with a model threshold M:

$$V_A = R - M.$$

Accordingly, a high model threshold indicates that accepting an offer has a low expected value.

The model threshold is computed in the following way:

$$M = c_1 + a \times c_2 - o \times c_3,$$

with c_1 being a constant threshold, a the number of offers accepted previously, o the offer index, and c_2 and c_3 as weight parameters for a and o, respectively. In this formulation, the model threshold increases linearly when a increases (since accept choices should be more conservative when many offers have already been accepted), and the model threshold decreases linearly when o increases (since accept choices should be more liberal when the end of a block is near).

Finally, the expected value of accepting V_A is used to compute the probability of accepting P_A via a sigmoid function:

$$P_A = \frac{1}{1 + \exp\left(-\tau \times V_A\right)}$$

with τ governing the slope of the probability distribution. Thus, the computational model has four free parameters: a constant value threshold (c_1), weight parameters for the number of accepts (c_2) and the number of offers (c_3), and a parameter for the slope of the sigmoid function (τ).

Invalid trials (i.e., in which the maximum number of offers were already accepted or no response was given in time) were not included in the model. To test for differences in task performance between the patient and control group, the following behavioral variables were analyzed: profit, mean reaction time, mean index of accepted offers (indicating how long subjects were willing to wait), parameter estimates of the computational decision model (c_1, c_2, and c_3), and mean model threshold (M). Group differences were tested via a general linear model (GLM) including a fixed factor for group membership (1 = controls, 2 = patients) and age as a covariate of no interest.

In addition to the analysis of behavioral data, the formula for the model threshold M and the decision value R were also used in fMRI analyses (as parametric modulators P2 and P1, see below). To identify neural correlates of these processes, the formula was applied for each trial based on the participant's extant behavior to that point in the block, to create an idealized value that was entered into the hemodynamic model as an idealized BOLD signal waveform.

MRI data acquisition and preprocessing

Functional data

Functional imaging was conducted in a 3 Tesla Siemens Tim Trio MRI scanner (Siemens, Erlangen, Germany) with a 12-channel head coil. 32 contiguous slices were acquired in ascending order using a T2*-weighted gradient-echo sequence. For each participant, 940 volumes were recorded with the following imaging parameters: repetition time (TR): 1.9 s; echo time (TE): 30 ms; matrix size: 64 × 64; field of view (FOV): 192 mm; flip angle: 80°; voxel size: 3.1 × 3.1 × 2.8 mm³; inter-slice gap: 0.7 mm.

TABLE 2 Behavioral data of alcohol-dependent patients and healthy control subjects

	Control subjects (23 male, nine female)		AD patients (22 male, 10 female)		Group difference[a]	
	Mean	SD	Mean	SD	F	p
Profit (cents; mean)	2725	134.6	2660.6	122.5	2.06	0.157
Index of accepted offers (mean)	10.5	1.2	10.2	1.5	0.47	0.498
Reaction time (ms; mean)	596.9	125.7	605.5	130.3	0.07	0.787
Model parameter c_1: constant value threshold	66.8	6	67.7	7	0.35	0.556
Model parameters c_2: number of accepts	3.1	1.4	3.1	1.2	0.01	0.908
Model parameter c_3: offer index	1.3	0.1	1.3	0.1	0.4	0.551
Model threshold M: (cents; mean)	59.3	3.8	60.2	4.9	1.25	0.268

[a]Group differences of behavioral data were analyzed via a GLM including a fixed factor for group membership and age as a covariate of no interest.

Structural data

For registration purposes, a high-resolution, T1-weighted structural scan was acquired from every subject with a three-dimensional magnetization prepared rapid gradient-echo sequence (192 slices; TR: 2.3 s; TE 3.03 ms, matrix size: 256 × 256; FOV: 256 mm; flip angle: 9°; voxel size: $1 \times 1 \times 1$ mm^3).

Preprocessing

The data were analyzed in Matlab (MathWorks) using SPM12 (Wellcome Department of Imaging Neuroscience, Institute of Neurology). Functional images were realigned to the first volume, slice-time corrected, coregistered to the structural data, spatially normalized to the template of the Montreal Neurological Institute (MNI), resampled to a voxel size of $3 \times 3 \times 3$ mm^3, and smoothed using a Gaussian kernel of 8 mm full-width at half-maximum.

fMRI data analysis

GLM analysis

The fMRI data were analyzed via a GLM for each participant. Different event regressors were constructed as box-car functions with onsets and durations of the respective choice periods:

Regressor R1 corresponded to the decision phase (Figure 1) of all trials for which participants made valid choices, excluding trials in which no response was given in the response phase, or trials for which offers could not be accepted anymore because the limit was already reached. To identify neural correlates of specific decision variables, linear parametric modulators of regressor R1 were included in the GLM for the offer value (P1) and the model threshold (P2). Thus, P1 comprises the raw monetary value of the offer, whereas P2 represents model-based decision processes that

take the offer index and the number of accepts into account. Both parametric modulators were z-transformed before they were added to the model. In addition, to minimize the error term of the GLM, regressors of no interest were included for the decision phase of invalid trials (R2), the response phase (R3), the feedback (R4), and pause (R5) phase between blocks, as well as six movement regressors R6 to R11 from the realignment procedure. R2 was included as a regressor of no interest because it is uncertain whether meaningful decision-making processes were present in invalid trials (since participants either did not indicate their choice in time or did not need to make a decision at all when they already accepted the maximum of five offers per block). Likewise, regressors R3 to R5 were of no interest since they were not part of the decision phase.

All regressors were convolved with the canonical hemodynamic response function and regressed against the BOLD signal in each voxel. Parametric modulators were not orthogonalized to each other, allowing regressors to fully compete for explained variance. First-level contrasts were constructed for offer values (P1) and model thresholds (P2) by weighting parametric modulators over baseline and submitted to second-level t-tests at the group level. One-sample t-tests were conducted separately for the patient and control group, and differential group effects were tested via two-sample t-tests that included age as a covariate of no interest. All statistical parametric maps from group analyses were thresholded at $p < 0.001$ (uncorrected) for voxel-level inference with a minimum cluster-size criterion of 10 contiguous voxels, and subsequent cluster-level family-wise error rate -correction for multiple testing at $p < 0.05$.

ROI analysis

ROIs were defined via spheres centered on coordinates from Economides et al. (2014). In particular, caudate nucleus ($x = -12$, $y = -6$, $z = 18$, radius = 5 mm) was used as an ROI for model-based decision processes, and vmPFC ($x = 4$, $y = 52$, $z = 14$, radius = 10 mm) as an ROI for value representation. Mean beta values of modulator P1

(offer value) and P2 (model threshold) were extracted from vmPFC and caudate nucleus, respectively. To analyze differences between groups, the beta values of each subject were entered into a GLM with a fixed factor for group membership and a covariate of no interest for age.

RESULTS

Behavioral results

Behavioral measures did not show significant group differences (Table 2), indicating that patients did not show impairments in task performance. In line with this result, summed accept responses for each trial in each block showed a similar distribution for both groups (Figure S1).

fMRI results

Whole-brain results

The first goal of the fMRI analysis was to identify regions that process the monetary value of offers. In the control group, whole-brain analyses revealed significant parametric modulation of offer values (P1) in a distributed set of regions including the dorsolateral prefrontal cortex (dlPFC), ventral striatum (vStr), and dorsomedial prefrontal cortex (dmPFC; Table 3; Figure 2A). The patient group showed activation in a largely overlapping set of regions (Table 3), and a whole-brain comparison of parametric group effects in a two-sample *t*-test did not reveal significant differences between the two groups.

Second, we investigated brain areas that demonstrated activation related to model-based decision processes via the model threshold parameter of the GLM (P2). In the control group, we did not observe effects related to positive model thresholds, but activity in the caudate nucleus and inferior parietal lobe was significantly associated with negative model thresholds (Table 3; Figure 2B), indicating stronger neural activity when the threshold was low and participants were more likely to accept offers. This is consistent with a previous study that found stronger effects for negative compared to positive model thresholds (Economides et al., 2014) and can be due to the BOLD signal being highest for go responses. The patient group, in contrast, did not show any activity related to negative model thresholds in the whole-brain analysis, but there was a significant cluster in the middle occipital gyrus associated with positive model thresholds (Table 3).

ROI results

ROI analyses were conducted to investigate group differences in vmPFC (associated with value representation) and caudate activation (associated with model-based decision processes). There were no group differences with respect to parametric effects of offer values in vmPFC, $F(1, 60) = 0.1$, $p_{FDR} = 0.834$), but we observed

a significant difference in parametric effects of model thresholds in caudate nucleus, $F(1, 60) = 4.4$, $p_{FDR} = 0.028$ (Figure 2C), with stronger negative beta values for the control group.

DISCUSSION

This study was designed to compare neural processes of value computation and model-based decision making between alcohol-dependent patients and healthy control subjects. Participants performed an fMRI decision task, in which monetary offers had to be evaluated with respect to dynamically changing constraints. The results showed that patients had decreased functional representation of model-based decision processes in the caudate nucleus, whereas there were no group differences in terms of neural value representation or task performance.

Previous studies have found that the caudate is a crucial area for the computation of goal-directed choices that require the consideration of multiple factors and long-term planning (Balleine & O'Doherty, 2010; Dolan & Dayan, 2013; Geerts et al., 2020; Sharpe et al., 2019; Wunderlich et al., 2012). Likewise, in rodents, model-based decision processes have been associated with signals in the dorsomedial striatum (Balleine, 2005; Corbit et al., 2012; Gahnstrom & Spiers, 2020), which corresponds to the caudate activation that human neuroscience studies have identified. Our finding that the neural representation of model-based decision processes in the caudate nucleus is decreased for patients only therefore suggests that AD impairs the neural computations in the medial dorsal striatum for goal-directed choices, and supports the hypothesis that the neural mechanism underlying the ability to flexibly adapt choices to long-term consequences is one of the core functions affected by the disorder (Bechara et al., 2001; Goudriaan et al., 2007; Reiter et al., 2016; Sebold et al., 2014, 2017). Surprisingly, the occipital gyrus was associated with positive model thresholds in patients. Although this region clearly is affected by AD (e.g., Hermann et al., 2007), so far little is known about its role in decision-making processes, which makes it an interesting research question for future studies.

Our data further revealed that offer value is represented in a distributed set of regions including vStr, dlPFC, and dmPFC for both the patient and the control group. However, we did not observe systematic differences with respect to neural value computations between the two groups. Previous studies have suggested that AD could be based on an overactive valuation system (Arcurio et al., 2015; Goldstein & Volkow, 2011; Seo et al., 2013). Since we did not observe systematic group differences with respect to neural value representations, the results of the current experiment do not support these hypotheses, and speak for a uniform processing of nonalcoholic stimulus values in patients and healthy controls. In line with that, Bjork et al. (2008) showed that reward and loss anticipation during a monetary incentive delay task elicited similar activation of vStr in patients and controls as well as similar mood responses. This finding underlines the notion that value representation might not be a characteristic marker of addiction.

TABLE 3 Brain regions showing task-related activation

Region	Side	MNI coordinates			T_{max}	p_{FWE} (cluster-level)
		x	Y	Z		
Controls						
Offer value						
Middle frontal gyrus	L	−24	−6	54	7.24	<0.001
Middle frontal gyrus	R	48	14	40	7.12	<0.001
Dorsolateral prefrontal cortex	R	44	40	24		
Dorsomedial prefrontal cortex	M	−2	30	42		
Ventral striatum	R	14	6	−6		
Inferior parietal lobe	R	40	−44	48	6.85	<0.001
Dorsolateral prefrontal cortex	L	−40	52	6	6.54	<0.001
Inferior parietal lobe	L	−44	−46	46	6.32	<0.001
Middle occipital gyrus	R	20	−94	10	5.26	<0.001
Cerebellum	L	−38	−66	−38	4.98	<0.001
Cerebellum	L	−12	−78	−34	4.96	<0.001
Middle occipital gyrus	L	−38	−92	0	4.95	<0.001
Substantia nigra	M	8	−18	−16	4.89	0.031
Negative model threshold						
Caudate	R	10	8	18	4.36	0.032
Inferior parietal lobe	L	42	−54	48	4.1	0.039
AD patients						
Offer value						
Dorsolateral prefrontal cortex	R	26	48	−8	6.51	<0.001
Dorsomedial prefrontal cortex	M	−2	32	38		
Ventral striatum	R	−10	10	−4		
Inferior parietal lobe	L	58	−44	50	5.65	<0.001
Cerebellum	L	−40	−72	−32	4.69	<0.001
Cerebellum	R	34	−56	−38	4.63	<0.001
Posterior cingulate cortex	M	4	−26	32	3.99	0.02
Model threshold						
Middle occipital gyrus		−30	−80	10	4.06	0.022

Note: Height threshold, T_{24} = 3.23; extent threshold, k_E = 10 voxels. All clusters survive whole-brain correction for multiple comparisons based on cluster-level FWE-control.

Interestingly, patients also did not show deviations in behavioral task performance. One explanation for this finding is that patients rely on different neural systems to achieve the same level of performance. Compensatory effects like these could also be found in other studies investigating decision making in AD patients (Charlet et al., 2014; Claus et al., 2018; Sebold et al., 2017), but the literature still shows mixed results (Galandra et al., 2018). The inconsistencies in the studies could result from the relatively large variance of decision-making tasks that were used since the tasks might recruit slightly different neural systems.

The absence of group differences in behavior and caudate responding could also be interpreted in the light of a finding by Gilman et al. (2015). They also observed that alcohol-dependent patients

and controls showed few differences in behavior or in mesolimbic activation by choice for and receipt of (risky) gains. Interestingly, a history of rewarded instrumental responses boosted the activation of motivational neurocircuitry for additional reward in terms that patients exhibited heightened striatal activation that correlated with total earnings during the task.

The lack of behavioral group differences in our data could be related to the novel decision-making paradigm that we used, which might not have been optimal to detect differences on the behavioral level. One could speculate that even though the neural differences in the caudate were not associated with behavioral group differences in our task, they could have been revealed with a decision task that includes more uncertainty and requires more complex long-term
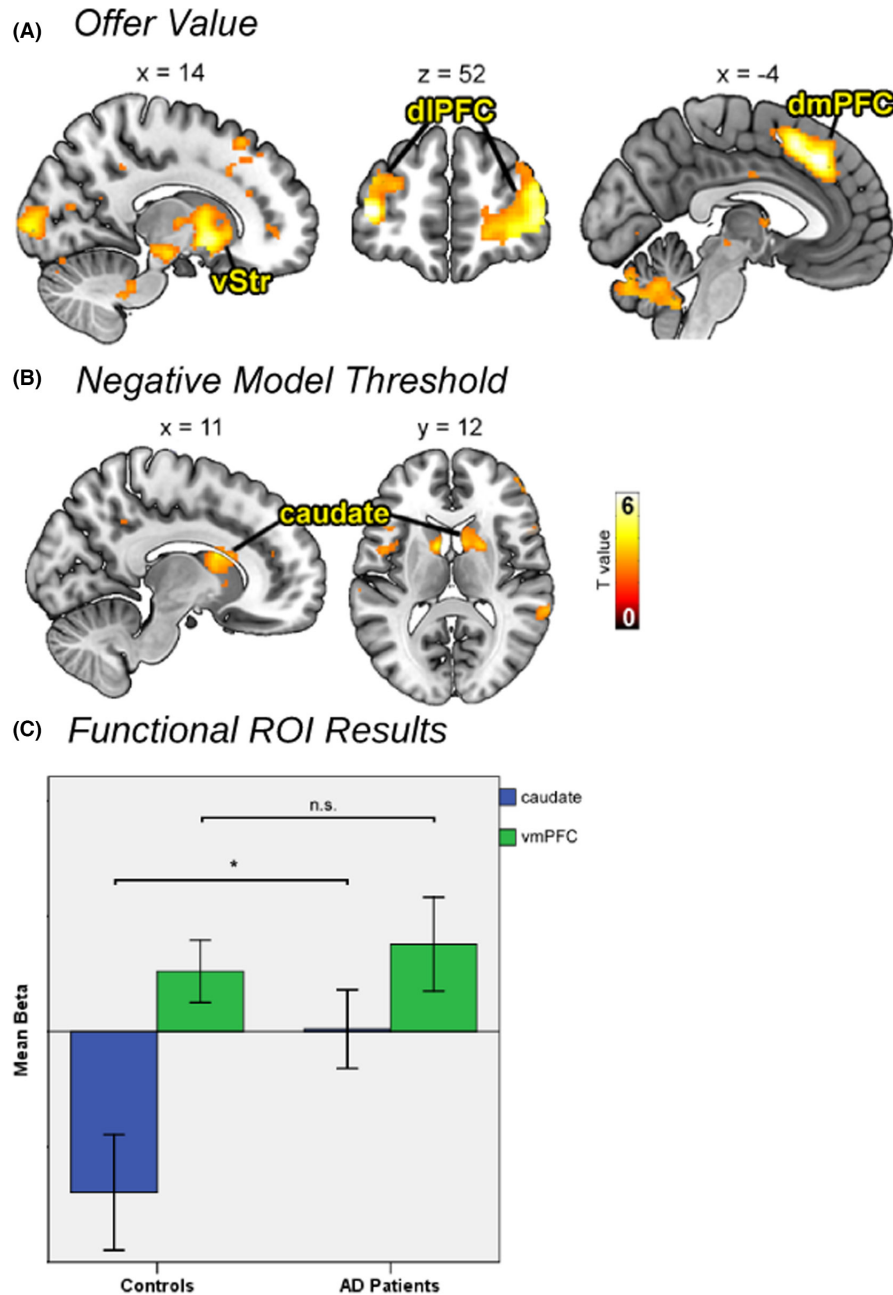
FIGURE 2 Brain regions showing parametric effects in the control group for (A) offer value and (B) negative model threshold. For illustration purposes, *t*-maps are thresholded at $p < 0.001$ (uncorrected), $k_E = 10$. Labelled clusters survive cluster-level FWE-correction at $p < 0.05$. The patient group showed largely overlapping clusters for offer values (Table 3), and no significant clusters for negative model thresholds. Abbreviations: dlPFC, dorsolateral prefrontal cortex; dmPFC, dorsomedial prefrontal cortex; vStr, ventral striatum. (C) Functional ROI results. Mean beta values in caudate nucleus were extracted from parametric modulators of model thresholds, and beta values in vmPFC from modulators of offer values, respectively. ROIs were defined as 5 mm spheres centered on coordinates from Economides et al. (2014). Asterisks denote significant FDR-corrected *p*-values < 0.05

planning. In the framework of our task, this could for example be tested in a future study by making trial-to-trial changes in monetary values more erratic, by increasing the number of trials per block, or by adding uncertainty to the number of offers that can be accepted (e.g., an unknown randomized number between 5 and 10 instead of the fixed number of 5).

Another limitation that has to be acknowledged in the interpretation of our study is that we did not control for nicotine dependence,

because it is significantly correlated with AD and would have interfered with the analysis of alcohol-related effects. Even though this is a common issue in the study of AD (Batel et al., 2006), it is a source of uncertainty that limits the strength of the conclusions that can be drawn.

To conclude, this study highlights the role of the caudate nucleus in computing goal-directed choices and integrating multiple factors into adaptive choices. AD patients showed a decreased functional

representation of model-based decision processes in this region, which could be a key factor that characterizes decision-making dysfunctions related to AD.

CONFLICT OF INTEREST

The authors declare no competing financial interests.

AUTHOR CONTRIBUTIONS

AM, CMS, and HW designed the study. AM was responsible for the data analysis, DJS conducted the computational modeling procedure, and all authors contributed to the discussion of the results. The manuscript was written by AM and edited by all authors.

ORCID

Amadeus Magrabi 🔗 https://orcid.org/0000-0002-1229-7708

REFERENCES

Amlung, M., Vedelago, L., Acker, J., Balodis, I. & MacKillop, J. (2017) Steep delay discounting and addictive behavior: a meta-analysis of continuous associations. *Addiction*, 112, 51–62. https://doi.org/10.1111/add.13535

Arcurio, L.R., Finn, P.R. & James, T.W. (2015) Neural mechanisms of high-risk decisions-to-drink in alcohol-dependent women. *Addiction Biology*, 20, 390–406. https://doi.org/10.1111/adb.12121

Balleine, B.W. (2005) Neural bases of food-seeking: affect, arousal and reward in corticostriatolimbic circuits. *Physiology & Behavior*, 86, 717–730. https://doi.org/10.1016/j.physbeh.2005.08.061

Balleine, B.W. & O'Doherty, J.P. (2010) Human and rodent homologies in action control: corticostriatal determinants of goal-directed and habitual action. *Neuropsychopharmacology*, 35, 48–69. https://doi.org/10.1038/npp.2009.131

Bartra, O., McGuire, J.T. & Kable, J.W. (2013) The valuation system: a coordinate-based meta-analysis of BOLD fMRI experiments examining neural correlates of subjective value. *NeuroImage*, 76, 412–427. https://doi.org/10.1016/j.neuroimage.2013.02.063

Batel, P., Pessione, F., Maître, C. & Rueff, B. (2006) Relationship between alcohol and tobacco dependencies among alcoholics who smoke. *Addiction*, 90, 977–980. https://doi.org/10.1046/j.1360-0443.1995.90797711.x

Bechara, A., Dolan, S., Denburg, N., Hindes, A., Anderson, S.W. & Nathan, P.E. (2001) Decision-making deficits, linked to a dysfunctional ventromedial prefrontal cortex, revealed in alcohol and stimulant abusers. *Neuropsychologia*, 39, 376–389. https://doi.org/10.1016/S0028-3932(00)00136-6

Beck, A., Wüstenberg, T., Genauck, A., Wrase, J., Schlagenhauf, F., Smolka, M.N. et al. (2012) Effect of brain structure, brain function, and brain connectivity on relapse in alcohol-dependent patients. *Archives of General Psychiatry*, 69, 842–852. https://doi.org/10.1001/archgenpsychiatry.2011.2026

Bjork, J.M., Smith, A.R. & Hommer, D.W. (2008) Striatal sensitivity to reward deliveries and omissions in substance dependent patients. *NeuroImage*, 42, 1609–1621. https://doi.org/10.1016/j.neuroimage.2008.06.035

Charlet, K., Beck, A., Jorde, A., Wimmer, L., Vollstädt-Klein, S., Gallinat, J. et al. (2014) Increased neural activity during high working memory load predicts low relapse risk in alcohol dependence. *Addiction Biology*, 19, 402–414. https://doi.org/10.1111/adb.12103

Chase, H.W., Eickhoff, S.B., Laird, A.R. & Hogarth, L. (2011) The neural basis of drug stimulus processing and craving: an activation likelihood estimation meta-analysis. *Biological Psychiatry*, 70, 785–793. https://doi.org/10.1016/j.biopsych.2011.05.025

Claus, E.D., Feldstein Ewing, S.W., Magnan, R.E., Montanaro, E., Hutchison, K.E. & Bryan, A.D. (2018) Neural mechanisms of risky decision making in adolescents reporting frequent alcohol and/or marijuana use. *Brain Imaging and Behavior*, 12, 564–576. https://doi.org/10.1007/s11682-017-9723-x

Clithero, J. & Rangel, A. (2014) Informatic parcellation of the network involved in the computation of subjective value. *Social Cognitive and Affective Neuroscience*, 9, 1289–1302. https://doi.org/10.1093/scan/nst106

Corbit, L.H., Nie, H. & Janak, P.H. (2012) Habitual alcohol seeking: time course and the contribution of subregions of the dorsal striatum. *Biological Psychiatry*, 72, 389–395. https://doi.org/10.1016/j.biopsych.2012.02.024

DePoy, L., Daut, R., Brigman, J.L., MacPherson, K., Crowley, N., Gunduz-Cinar, O. et al. (2013) Chronic alcohol produces neuroadaptations to prime dorsal striatal learning. *Proceedings of the National Academy of Sciences of the United States of America*, 110, 14783–14788. https://doi.org/10.1073/pnas.1308198110

Dolan, R.J. & Dayan, P. (2013) Goals and habits in the brain. *Neuron*, 80, 312–325. https://doi.org/10.1016/j.neuron.2013.09.007

Economides, M., Guitart-Masip, M., Kurth-Nelson, Z. & Dolan, R.J. (2014) Anterior cingulate cortex instigates adaptive switches in choice by integrating immediate and delayed components of value in ventromedial prefrontal cortex. *Journal of Neuroscience*, 34, 3340–3349. https://doi.org/10.1523/JNEUROSCI.4313-13.2014

Everitt, B.J. & Robbins, T.W. (2005) Neural systems of reinforcement for drug addiction: from actions to habits to compulsion. *Nature Neuroscience*, 8, 1481–1489. https://doi.org/10.1038/nn1579

Everitt, B.J. & Wolf, M.E. (2002) Psychomotor stimulant addiction: a neural systems perspective. *Journal of Neuroscience*, 22, 3312–3320.

First, M., Spitzer, R., Gibbon, M. & Williams, J. (2001) *Structured clinical interview for DSM-IV-TR Axis I disorders, research version, patient edition with psychotic screen (SCID-I/PW/PSY SCREEN)*. New York: New York State Psychiatric Institute, Biometrics Research.

Furlong, T.M., Jayaweera, H.K., Balleine, B.W. & Corbit, L.H. (2014) Binge-like consumption of a palatable food accelerates habitual control of behavior and is dependent on activation of the dorsolateral striatum. *Journal of Neuroscience*, 34, 5012–5022. https://doi.org/10.1523/JNEUROSCI.3707-13.2014

Gahnstrom, C.J. & Spiers, H.J. (2020) Striatal and hippocampal contributions to flexible navigation in rats and humans. *Brain and Neuroscience Advances*, 4, 1–7. https://doi.org/10.1177/2398212820979772

Galandra, C., Basso, G., Cappa, S. & Canessa, N. (2018) The alcoholic brain: neural bases of impaired reward-based decision-making in alcohol use disorders. *Neurological Sciences*, 39, 423–435. https://doi.org/10.1007/s10072-017-3205-1

Geerts, J.P., Chersi, F., Stachenfeld, K.L. & Burgess, N. (2020) A general model of hippocampal and dorsal striatal learning and decision making. *Proceedings of the National Academy of Sciences of the United States of America*, 117, 31427–31437. https://doi.org/10.1073/pnas.2007981117

Gilman, J.M., Smith, A.R., Bjork, J.M., Ramchandani, V.A., Momenan, R. & Hommer, D.W. (2015) Cumulative gains enhance striatal response

to reward opportunities in alcohol-dependent patients. *Addiction Biology*, 20, 580–593. https://doi.org/10.1111/adb.12147

Goldstein, R.Z. & Volkow, N.D. (2011) Dysfunction of the prefrontal cortex in addiction: neuroimaging findings and clinical implications. *Nature Reviews Neuroscience*, 12, 652–669. https://doi.org/10.1038/nrn3119

Goudriaan, A.E., Grekin, E.R. & Sher, K.J. (2007) Decision making and binge drinking: a longitudinal study. *Alcoholism, Clinical and Experimental Research*, 31, 928–938. https://doi.org/10.1111/j.1530-0277.2007.00378.x

Hermann, D., Smolka, M.N., Klein, S., Heinz, A., Mann, K. & Braus, D.F. (2007) Reduced fMRI activation of an occipital area in recently detoxified alcohol-dependent patients in a visual and acoustic stimulation paradigm. *Addiction Biology*, 12, 117–121. https://doi.org/10.1111/j.1369-1600.2006.00039.x

Kamarajan, C., Ardekani, B.A., Pandey, A.K., Kinreich, S., Pandey, G., Chorlian, D.B. et al. (2020) Random forest classification of alcohol use disorder using fMRI functional connectivity, neuropsychological functioning, and impulsivity measures. *Brain Sciences*, 10, 115. https://doi.org/10.3390/brainsci10020115

Koob, G.F. & Volkow, N.D. (2010) Neurocircuitry of addiction. *Neuropsychopharmacology*, 35, 217–238. https://doi.org/10.1038/npp.2009.110

Kühn, S. & Gallinat, J. (2011) Common biology of craving across legal and illegal drugs—a quantitative meta-analysis of cue-reactivity brain response. *European Journal of Neuroscience*, 33, 1318–1326. https://doi.org/10.1111/j.1460-9568.2010.07590.x

Lee, S., Yu, L.Q., Lerman, C. & Kable, J.W. (2021) Subjective value, not a gridlike code, describes neural activity in ventromedial prefrontal cortex during value-based decision-making. *NeuroImage*, 237, 118159. https://doi.org/10.1016/j.neuroimage.2021.118159

Luijten, M., Schellekens, A.F., Kühn, S., Machielse, M.W. & Sescousse, G. (2017) Disruption of reward processing in addiction: an image-based meta-analysis of functional magnetic resonance imaging studies. *JAMA Psychiatry*, 74, 387–398. https://doi.org/10.1001/jamapsychiatry.2016.3084

Mollick, J.A. & Kober, H. (2020) Computational models of drug use and addiction: a review. *Journal of Abnormal Psychology*, 129, 544–555. https://doi.org/10.1037/abn0000503

Phung, Q.H., Snider, S.E., Tegge, A.N. & Bickel, W.K. (2019) Willing to work but not to wait: individuals with greater alcohol use disorder show increased delay discounting across commodities and less effort discounting for alcohol. *Alcoholism: Clinical and Experimental Research*, 43, 927–936. https://doi.org/10.1111/acer.13996

Reiter, A.M.F., Deserno, L., Kallert, T., Heinze, H.-J., Heinz, A. & Schlagenhauf, F. (2016) Behavioral and neural signatures of reduced updating of alternative options in alcohol-dependent patients during flexible decision-making. *Journal of Neuroscience*, 36, 10935–10948. https://doi.org/10.1523/JNEUROSCI.4322-15.2016

Rubio, G., Jiménez, M., Rodríguez-Jiménez, R., Martínez, I., Avila, C., Ferre, F. et al. (2008) The role of behavioral impulsivity in the development of alcohol dependence: a 4-year follow-up study. *Alcoholism, Clinical and Experimental Research*, 32, 1681–1687. https://doi.org/10.1111/j.1530-0277.2008.00746.x

Schacht, J.P., Anton, R.F. & Myrick, H. (2013) Functional neuroimaging studies of alcohol cue reactivity: a quantitative meta-analysis and systematic review. *Addiction Biology*, 18, 121–133. https://doi.org/10.1111/j.1369-1600.2012.00464.x

Schad, D.J., Garbusow, M., Friedel, E., Sommer, C., Sebold, M., Hägele, C. et al. (2019) Neural correlates of instrumental responding in the context of alcohol-related cues index disorder severity and relapse risk. *European Archives of Psychiatry and Clinical Neuroscience*, 269, 295–308. https://doi.org/10.1007/s00406-017-0860-4

Sebold, M., Deserno, L., Nebe, S., Nebe, S., Schad, D.J., Garbusow, M. et al. (2014) Model-based and model-free decisions in alcohol dependence. *Neuropsychobiology*, 70, 122–131. https://doi.org/10.1159/000362840

Sebold, M., Nebe, S., Garbusow, M., Guggenmos, M., Schad, D.J., Beck, A. et al. (2017) When habits are dangerous: alcohol expectancies and habitual decision making predict relapse in alcohol dependence. *Biological Psychiatry*, 82, 847–856. https://doi.org/10.1016/j.biopsych.2017.04.019

Seo, D., Lacadie, C.M., Tuit, K., Hong, K.-I., Constable, R.T. & Sinha, R. (2013) Disrupted ventromedial prefrontal function, alcohol craving, and subsequent relapse risk. *JAMA Psychiatry*, 70, 727–739. https://doi.org/10.1001/jamapsychiatry.2013.762

Sharpe, M.J., Stalnaker, T., Schuck, N.W., Killcross, S., Schoenbaum, G. & Niv, Y. (2019) An integrated model of action selection: distinct modes of cortical control of striatal decision making. *Annual Review of Psychology*, 70, 53–76. https://doi.org/10.1146/annurev-psych-010418-102824

Skinner, H.A. & Sheu, W.J. (1982) Reliability of alcohol use indices. The lifetime drinking history and the MAST. *Journal of Studies on Alcohol*, 43, 1157–1170. https://doi.org/10.15288/jsa.1982.43.1157

Spanagel, R., Bartsch, D., Brors, B., Dahmen, N., Deussing, J., Eils, R. et al. (2010) An integrated genome research network for studying the genetics of alcohol addiction. *Addiction Biology*, 15, 369–379. https://doi.org/10.1111/j.1369-1600.2010.00276.x

Virkkunen, M. (1994) Personality profiles and state aggressiveness in finnish alcoholic, violent offenders, fire setters, and healthy volunteers. *Archives of General Psychiatry*, 51, 28. https://doi.org/10.1001/archpsyc.1994.03950010028004

Vollstädt-Klein, S., Wichert, S., Rabinstein, J., Bühler, M., Klein, O., Ende, G. et al. (2010) Initial, habitual and compulsive alcohol use is characterized by a shift of cue processing from ventral to dorsal striatum. *Addiction*, 105, 1741–1749. https://doi.org/10.1111/j.1360-0443.2010.03022.x

Voon, V., Reiter, A., Sebold, M. & Groman, S. (2017) Model-based control in dimensional psychiatry. *Biological Psychiatry*, 82, 391–400. https://doi.org/10.1016/j.biopsych.2017.04.006

World Health Organization. (2018) *World Health Statistics*. Geneva: WHO.

Wrase, J., Schlagenhauf, F., Kienast, T., Wüstenberg, T., Bermpohl, F., Kahnt, T. et al. (2007) Dysfunction of reward processing correlates with alcohol craving in detoxified alcoholics. *NeuroImage*, 35, 787–794. https://doi.org/10.1016/j.neuroimage.2006.11.043

Wunderlich, K., Dayan, P. & Dolan, R.J. (2012) Mapping value based planning and extensively trained choice in the human brain. *Nature Neuroscience*, 15, 786–791. https://doi.org/10.1038/nn.3068

Yin, H.H., Knowlton, B.J. & Balleine, B.W. (2004) Lesions of dorsolateral striatum preserve outcome expectancy but disrupt habit formation in instrumental learning. *European Journal of Neuroscience*, 19, 181–189. https://doi.org/10.1111/j.1460-9568.2004.03095.x

Yin, H.H., Ostlund, S.B., Knowlton, B.J. & Balleine, B.W. (2005) The role of the dorsomedial striatum in instrumental conditioning. *European Journal of Neuroscience*, 22, 513–523. https://doi.org/10.1111/j.1460-9568.2005.04218.x

SUPPORTING INFORMATION

Additional supporting information may be found in the online version of the article at the publisher's website.